

GA-A26808

ELECTRON COLLISIONS IN THE TRAPPED GYRO-LANDAU FLUID TRANSPORT MODEL

by
G.M. STAEBLER and J.E. KINSEY

SEPTEMBER 2010



DISCLAIMER

This report was prepared as an account of work sponsored by an agency of the United States Government. Neither the United States Government nor any agency thereof, nor any of their employees, makes any warranty, express or implied, or assumes any legal liability or responsibility for the accuracy, completeness, or usefulness of any information, apparatus, product, or process disclosed, or represents that its use would not infringe privately owned rights. Reference herein to any specific commercial product, process, or service by trade name, trademark, manufacturer, or otherwise, does not necessarily constitute or imply its endorsement, recommendation, or favoring by the United States Government or any agency thereof. The views and opinions of authors expressed herein do not necessarily state or reflect those of the United States Government or any agency thereof.

GA-A26808

ELECTRON COLLISIONS IN THE TRAPPED GYRO-LANDAU FLUID TRANSPORT MODEL

by
G.M. STAEBLER and J.E. KINSEY

This is a preprint of a paper to be to be submitted for
publication in *Physics of Plasmas*.

Work supported by
the U.S. Department of Energy
under DE-FG02-95ER54309

**GENERAL ATOMICS ATOMICS PROJECT 03726
SEPTEMBER 2010**



ABSTRACT

Accurately modeling electron collisions in the trapped gyro-Landau fluid (TGLF) equations has been a major challenge. Insights gained from numerically solving the gyro-kinetic equation have led to a significant improvement of the low order TGLF model. The theoretical motivation and verification of this model with the velocity-space gyro-kinetic code GYRO [J. Candy and R.E. Waltz, *J. Comp. Physics* **186**, 545 (2003)] will be presented. The improvement in the fidelity of TGLF to GYRO is shown to also lead to better prediction of experimental temperature profiles by TGLF for a dedicated collision frequency scan.

I. INTRODUCTION

The literature on the theory of electron collisions (electron-electron and electron-ion) in the gyro-kinetic equation is long and rich with specific models developed to suit the solution technique employed. Here we are interested in the fluid moment closures of the gyro-kinetic equation that began with the work of Hammett and Perkins¹ on the Landau-fluid closure and progressed to gyro-Landau fluids (GLF) which include toroidal drifts.²⁻⁶ In particular, this paper reports the development of the electron collision model in the trapped gyro-Landau fluid (TGLF) equations⁷ that include trapped particles in a unified way. All of these fluid models use complex closures to retain the kinetic effects of the Landau and curvature drift poles in the linear gyro-kinetic response function. The fluid closure coefficients are chosen to give the best fit to the local kinetic linear density response. This procedure is done without collisions. It is not trivial to include collisions in this method. A differential equation in velocity space needs to be solved in order to obtain a kinetic response function to fit the fluid closure to. It is not necessary to change the collisionless TGLF model (closures⁷ or saturation rule⁸) in order to add collisions. The collision model closures are independent of the other closures employed. Previous GLF models have included electron collisions. The GLF23⁶ system of equations used a model for the collisional exchange of particles across the trapped-passing boundary. The bounce averaged trapped electron equations of Beer and Hammett⁵ include collisions as a differential operator.

In this paper, we will start with the case of no-trapping. A numerical solution for the linear kinetic response function with pitch-angle scattering will be used to determine the best-fit fluid moment coefficients for collision terms. The pitch angle scattering differential form of the electron collision operator has been used in numerical velocity space solutions of the gyro-kinetic equation.^{9,10} These initial-value solutions were used to verify the TGLF linear stability results.

Next the case with trapped electrons will be addressed. A model for the averaging of the Landau resonance by trapped electrons is introduced to obtain the kinetic solution. Fitting TGLF to this kinetic response did not yield a good fit to the initial-value gyro-kinetic results so the averaging model is suspect. However, the insights gained from the kinetic solution with trapped particles did lead to a better TGLF model which was the ultimate goal. In particular, the kinetic solution resolved the issue of what the high collision frequency limit of the trapped electron response should be in TGLF.

Finally, the verification of the new collision model in TGLF with non-linear GYRO¹⁰ turbulence simulations will be presented. The new model greatly improves the fidelity to GYRO compared to the previous one used for testing TGLF with experimental data.⁸ The new model does not change the overall statistical agreement of TGLF predicted temperatures with the large dataset of data used in Ref. 8 but it will be shown to improve the agreement with a dedicated experiment designed to change only the collisionality keeping other dimensionless plasma parameters fixed.

II. WITHOUT TRAPPED PARTICLES

The gyro-kinetic equation¹¹ is valid for frequencies that are small compared to the gyro-frequency of the species. For poloidal wavelengths longer than the ion gyro-radius $k_\theta \rho_i < 1$, the electron Landau resonance frequency $\omega_L = \sqrt{T_e/m_e} k_\parallel$ is typically much larger than the diamagnetic or curvature drift frequencies. Hence, it is sufficient for the purpose of determining the collision model to take the limit $k_\theta \rho_e \rightarrow 0$ of the circulating electron equation. For trapped electron instabilities, the mode frequency needs to be less than the Landau resonance frequency so that the bounce motion of the electrons can average away the Landau resonance. The impact of electron collisions is to couple the trapped and passing electrons. Hence, only the largest term in the passing equation (the Landau resonance frequency) needs to be included in the kinetic model to be solved for the density response function. The gyro-kinetic equation for passing electrons with a Maxwellian background distribution function in the low-beta approximation and taking $k_\theta \rho_e \rightarrow 0$ reduces to (suppressing the electron species label)

$$-i\omega g - ik_p \xi g - C(g) = i\omega \Phi F_0(E) \quad , \quad (1)$$

where

$$\xi = v_\parallel / v, \quad \Phi = e\tilde{\phi}/T, \quad F_0 = [n_0 / (2\pi v_t^2)^{3/2}] e^{-E}, \quad k_p = \sqrt{2E}\omega_L, \quad v_t = \sqrt{T/m}, \quad E = v^2 / 2v_t^2, \quad \omega_L = k_\parallel v_t.$$

Neglecting the ion momentum restoring terms for simplicity, the pitch angle scattering collision operator¹² including both electron-electron ($Z_{eff} = 0$ term) and electron-ion collisions ($Z_{eff} > 0$ term) is $C(g) = (v_E/2)(\partial/\partial\xi)(1-\xi^2)(\partial/\partial\xi)g$ with an energy dependent scattering rate

$$v_E = \frac{v_e}{E^{3/2}} \left[Z_{eff} + \frac{e^{-E}}{\sqrt{\pi E}} + \left(1 - \frac{1}{2E}\right) \text{Erf}\left(E^{1/2}\right) \right] \quad , \quad (2)$$

$$\text{and } v_e = 4\pi n_e e^4 \ln(\Lambda) / (2^{3/2} v_{te}^3 m_e^2), \quad Z_{eff} = \sum_{a=ions} z_a^2 n_a / n_e.$$

The first order gyro-phase independent part of the fluctuating distribution function g is defined in Ref. 11. Expanding g in a finite series of Legendre polynomials in ξ , (a natural choice that diagonalizes the pitch-angle collision operator)

$$g = \sum_{n=0}^{N_{max}} g_n(E) P_n(\xi) \quad . \quad (3)$$

Equation (1) can be solved for the coefficients g_n . The kinetic density response function is defined by

$$R_N^{kin} = 1 - N/\Phi \quad \text{where} \quad N = \int d^3v g / n_0 \quad . \quad (4)$$

For at least 24 Legendre polynomials, an accurate agreement between this kinetic model and the analytic result⁷ is obtained for small growth rate $\text{Im}[\omega]=0.01\omega_L$ and small collision frequency $\nu_e=0.01\omega_L$.

The TGLF moment equations⁷ can be considered a special case of the above Legendre polynomial expansion with $N_{\max}=5$ and the energy dependence of the coefficients prescribed by

$$g_0 = \left[NL_0^{1/2}(E) - TL_1^{1/2}(E) + dR_{T,T} \frac{3}{5} L_2^{1/2}(E) \right] F_0 \quad , \quad (5a)$$

$$g_1 = \left[U_{\parallel} L_0^{3/2}(E) - q_T \frac{3}{5} L_1^{3/2}(E) + dS_{T,T} \frac{9}{35} L_2^{3/2}(E) \right] \sqrt{2E} F_0 \quad , \quad (5b)$$

$$g_2 = \left[\Pi L_0^{5/2}(E) - dR_{\parallel,T} \frac{3}{7} L_1^{5/2}(E) \right] E F_0 \quad , \quad (5c)$$

$$g_3 = \left[\Theta \frac{1}{3} L_0^{7/2}(E) - dS_{\parallel,T} \frac{1}{9} L_1^{7/2}(E) \right] \sqrt{2E} E F_0 \quad , \quad (5d)$$

$$g_4 = dR_{\parallel,\parallel} \frac{1}{6} L_0^{9/2}(E) E^2 F_0 \quad , \quad (5e)$$

$$g_5 = dS_{\parallel,\parallel} L_0^{11/2}(E) \sqrt{2E} \frac{E^2}{30} F_0 \quad . \quad (5f)$$

Where $L_n^a(E)$ are the generalized Leguerre polynomials. The six moments evolved by the TGLF equations in the $k_{\theta}\rho_e \rightarrow 0$ limit are

$$N = \frac{1}{n_0} \int d^3v P_0(\xi) L_0^{1/2}(E) g \quad , \quad (6a)$$

$$T = -\frac{2}{3} \frac{m}{n_0 v_t^2} \int d^3v P_0(\xi) L_1^{1/2}(E) g \quad , \quad (6b)$$

$$U_{\parallel} = \frac{1}{n_0 v_t} \int d^3v P_1(\xi) L_0^{3/2}(E) \sqrt{2E} g \quad , \quad (6c)$$

$$q_T = -\frac{2}{3} \frac{1}{n_0 v_t^3} \int d^3v P_1(\xi) L_1^{3/2}(E) \sqrt{2E} g \quad , \quad (6d)$$

$$\Pi = \frac{4}{3} \frac{1}{n_0 v_t^2} \int d^3v P_2(\xi) L_0^{5/2}(E) E g \quad , \quad (6e)$$

$$\Theta = \frac{4}{5} \frac{1}{n_0 v_t^3} \int d^3v P_3(\xi) L_0^{7/2}(E) \sqrt{2E} E g \quad . \quad (6f)$$

The higher velocity moments are closed in various ways for different limits

$$dR_{T,T} = \frac{8}{9} \frac{1}{n_0 v_t^4} \int d^3 v P_0(\xi) L_2^{1/2} g \quad , \quad (7a)$$

$$dS_{T,T} = \frac{8}{9} \frac{1}{n_0 v_t^5} \int d^3 v P_1(\xi) L_2^{3/2}(E) \sqrt{2E} g \quad , \quad (7b)$$

$$dR_{\parallel,T} = -\frac{8}{9} \frac{1}{n_0 v_t^4} \int d^3 v P_2(\xi) L_1^{5/2}(E) E g \quad , \quad (7c)$$

$$dS_{\parallel,T} = -\frac{8}{15} \frac{1}{n_0 v_t^5} \int d^3 v P_3(\xi) L_1^{7/2}(E) \sqrt{2E} E g \quad , \quad (7d)$$

$$dR_{\parallel,\parallel} = \frac{32}{35} \frac{1}{n_0 v_t^4} \int d^3 v P_4(\xi) L_0^{9/2}(E) E^2 g \quad . \quad (7e)$$

$$dS_{\parallel,\parallel} = \frac{32}{63} \frac{1}{n_0 v_t^5} \int d^3 v P_5(\xi) L_0^{11/2}(E) \sqrt{2E} E^2 g \quad . \quad (7f)$$

These moments are normalized so as to have a simple mapping to the moments used in Ref. 7.

The TGLF moment equations (in the $k_\theta \rho_e \rightarrow 0$ limit) without trapped particles are total velocity space moments of Eq. (1). Grouping terms corresponding to Legendre coefficients they can be written

$$-i\omega N + i\omega \Phi + i\omega_L U_{\parallel} = 0 \quad , \quad (8a)$$

$$i\omega T + i\omega_L \left(q_T + \frac{2}{3} U_{\parallel} \right) = 0 \quad , \quad (8b)$$

$$-i\omega U_{\parallel} + i\omega_L (\Pi + T + N) = -\nu_{U1} U_{\parallel} - \nu_{U2} q_T - \nu_{U3} dS_{T,T} \quad , \quad (8c)$$

$$-i\omega q_T + i\omega_L \left(dR_{\parallel,T} + dR_{TT} + \frac{2}{3} \Pi + \frac{5}{3} T \right) = -\nu_{Q1} U_{\parallel} - \nu_{Q2} q_T - \nu_{Q3} dS_{T,T} \quad , \quad (8d)$$

$$-i\omega \Pi + i\omega_L \left(\Theta + \frac{4}{5} q_T + \frac{4}{3} U_{\parallel} \right) = -\nu_{\Pi1} \Pi - \nu_{\Pi2} dR_{\parallel,T} \quad , \quad (8e)$$

$$-i\omega \Theta + i\omega_L \left(dR_{\parallel,\parallel} + \frac{27}{35} dR_{\parallel,T} + \frac{9}{5} \Pi \right) = -\nu_{\Theta1} \Theta - \nu_{\Theta2} dS_{\parallel,T} \quad . \quad (8f)$$

The first two are from the P_0 moment, the 3rd and 4th are from P_1 the 5th is from P_2 and the 6th equation is from P_3 . In the collisionless limit, the highest irreducible moments ($dR_{T,T}$, $dR_{\parallel,T}$, $dR_{\parallel,\parallel}$) on the left hand side are closed using the Landau-fluid closures.^{1,3} In the high

collision frequency limit $\nu_{ei} \gg \nu_t k_{\parallel}$, the highest moments on the right hand side will be closed by the relations

$$dS_{T,T} = \alpha_{10} U_{\parallel} + \alpha_{11} q_T \quad , \quad (9a)$$

$$dR_{\parallel,T} = \alpha_{20} \Pi \quad , \quad (9b)$$

$$dS_{\parallel,T} = \alpha_{30} \Theta \quad . \quad (9c)$$

This form of closure writes the higher irreducible energy moments in terms of the lower energy moments of the same Legendre harmonic. The net result is that the collision coefficient for the lower energy moments become renormalized and can be used as fitting parameters to improve the model fidelity to the kinetic response function. With this closure, the TGLF equations become

$$-i\omega N + i\omega\Phi + i\omega_L U_{\parallel} = 0 \quad , \quad (10a)$$

$$-i\omega T + i\omega_L \left(q_T + \frac{2}{3} U_{\parallel} \right) = 0 \quad (10b)$$

$$-i\omega U_{\parallel} + i\omega_L (\Pi + T + N) = -\nu_{UU} U_{\parallel} - \nu_{UQ} q_T \quad , \quad (10c)$$

$$-i\omega q_T + i\omega_L \left(dR_{\parallel,T}^{LF} + dR_{TT}^{LF} + \frac{2}{3} \Pi + \frac{5}{3} T \right) = -\nu_{QU} U_{\parallel} - \nu_{QQ} q_T \quad , \quad (10d)$$

$$-i\omega \Pi + i\omega_L \left(\Theta + \frac{4}{5} q_T + \frac{4}{3} U_{\parallel} \right) = -\nu_{\Pi} \Pi \quad , \quad (10e)$$

$$-i\omega \Theta + i\omega_L \left(dR_{\parallel,\parallel}^{LF} + \frac{27}{35} dR_{\parallel,T}^{LF} + \frac{9}{5} \Pi \right) = -\nu_{\Theta} \Theta \quad . \quad (10f)$$

Where the superscript LF refers to the Landau-fluid closure^{1,3} form for these moments.⁷ The collision coefficients can be written in the form

$$\nu_{\Pi} = \nu_e \frac{4}{5} K_4 \quad , \quad (11a)$$

$$\nu_{UQ} = \nu_e \left(\frac{2}{5} K_2 - K_1 \right) \quad , \quad (11b)$$

$$\nu_{UU} = \nu_e \frac{2}{3} K_1 \quad , \quad (11c)$$

$$\nu_{QQ} = \nu_e \left(\frac{4}{15} K_3 - \frac{4}{3} K_2 + \frac{5}{3} K_1 \right) \quad , \quad (11d)$$

$$\nu_{\Theta} = \nu_e \frac{16}{35} K_5 \quad , \quad (11e)$$

$$\nu_{QU} = \frac{9}{10} \nu_{UQ} \quad . \quad (11f)$$

where

$$\begin{aligned} K_1 &= c_1 + Z_{eff} c_2, & K_2 &= c_3 + Z_{eff} c_4, & K_3 &= c_5 + Z_{eff} c_6, \\ K_4 &= c_7 + Z_{eff} c_8, & K_5 &= c_9 + Z_{eff} c_{10}. \end{aligned} \quad (12)$$

An alternative closure for the collision terms is to set the irreducible higher energy moments ($dR_{\parallel,T}$, $dS_{T,T}$, $dS_{\parallel,T}$) to zero. This will be referred to as the truncation case. In this case, the $K(s)$ are energy integrals of the scattering rate function ν_E/ν_e weighted with different powers of the energy. The truncated case coefficient values are listed in Table I. Only three $K(s)$ are independent with $K_4 = K_1$ and $K_5 = K_3$ for the truncated case. Note that the Onsager symmetry with respect to the energy moments constrains the ν_{QU} term.

Table I
Collision Coefficients for Circulating Electrons

Coefficient:	c1	c2	c3	c4	c5	c6	c7	c8	c9	c10
Truncation:	0.601	1.128	0.798	1.128	1.795	2.257	0.601	1.128	1.795	2.257
Optimized:	0.492	0.754	0.673	0.805	1.627	2.013	0.497	0.781	1.694	3.103

Computing the response function for the TGLF moment equations and performing a conjugate gradient iteration of the collision coefficients (c_1, \dots, c_{10}) to minimize the error between the TGLF response functions and the numerically evaluated kinetic response functions gives the set of optimized coefficients in Table I.

An illustration of the quality of fit is shown in Fig. 1 for 32 Legendre polynomials. This is in the transition region $\nu_e = \omega_L$ where the TGLF model is the least accurate. The optimized fit closure coefficients somewhat improve the fit of the TGLF model to the kinetic result (5.8% deviation) compared with the truncated evaluation of the coefficients (6.3% deviation). These deviations are averaged over ($\nu_{ei}/\omega_L = 0.01, 0.05, 0.1, 0.5, 1.0, 5.0, 50.0$; $Z_{eff} = 0, 2$) and a range of 32 frequencies at $\text{Im}[\omega] = 0.01\omega_L$. The deviations from the four moments (N, U_{\parallel}, T, q_T) needed to compute fluxes are included in the average deviation. These optimized coefficients will be used for the circulating particle sector of the TGLF model with trapped particles.

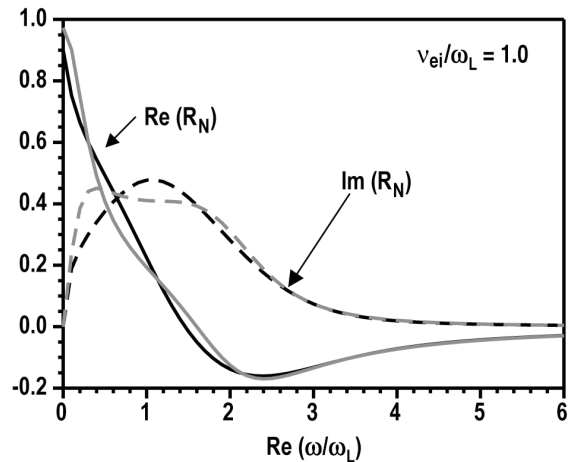


Fig. 1. Real (solid) and imaginary (dashed) parts of the density response function for $\nu_{ei}/\omega_L = 1$, showing kinetic solution with 32 Legendre Polynomials (black) and TGLF optimized model (gray).

III. WITH TRAPPED PARTICLES

Including trapped particles in the kinetic solution is not straight forward. Simply adding the mirror force term arising from the commutator of the parallel gradient operator with the parallel velocity (for fixed energy and magnetic moment) does not capture the most important aspect of the trapped particle response, the bounce averaging of the Landau resonance. In fact, the mirror force term has very little impact on the density response function and will be neglected. In the collisionless limit, it can be shown⁷ that setting the odd velocity moments and parallel gradients to zero, and taking velocity moments only in the trapped region, yields the same density response function as obtained from the bounce averaged kinetic equation.⁵ In order for the kinetic solution with collisions to recover the collisionless limit, some model for the impact of the bounce averaging of the Landau resonance is required. There is no need for a “bounce averaging model” for initial value solutions to the kinetic equations. It is only because we are trying to work with the Fourier transform of the gyro-kinetic equation into frequency, which involves integration over time, that the dynamic bounce averaging must be modeled.

One model for the bounce averaging with collisions has been proposed in Ref. 13. Here the trapped-passing boundary used for the integration domain is modified by the collisions. The collisions de-trap the particles preferentially in the low energy corner of velocity space due to the $E^{-3/2}$ dependence of the scattering rate. This model can be implemented in velocity moment equations like TGLF and was extensively tested by us. The short answer is that it does not give linear growth rates that agree with the initial value solutions of the full gyro-kinetic equations with pitch angle scattering such as GYRO.¹⁰ This model gives an effective trapped region boundary that depends on the well known parameter $\nu^* = \nu_e R q / (\nu_{the} \epsilon^{3/2})$. It is found that this model gives the wrong dependence of the linear growth rates on the local aspect ratio $\epsilon = r/R$ and the safety factor q compared to the GYRO results. The parameter ν_e / ω_L has already been shown to be a natural dimensionless metric for the circulating electrons. This has a weaker q -dependence than ν^* since the parallel mode width shrinks with increasing q . It also has a different aspect ratio dependence than ν^* .

The model for bounce averaging that will be used to compute the kinetic response functions is similar to the model used in TGLF.⁷ It will be assumed that, within the trapped region, all of the odd moments of the distribution function and the k_{\parallel} operator vanish. This prescription has been shown to exactly reproduce the bounce averaged response in the collisionless limit. The distribution function can still be represented by a finite expansion of Legendre Polynomials that are continuous across the trapped-passing boundary. Defining the passing region projection operator as

$$A\{\xi\} = \begin{cases} \xi & \text{if } |\xi| \geq f_t \\ 0 & \text{if } |\xi| < f_t \end{cases} . \quad (13)$$

Where $f_t = \sqrt{1 - B(\theta)/B_{\max}}$ is the local trapped-passing boundary value of $|\xi|$.

We can write the distribution function as a sum of even and odd parts where

$$g_{\text{even}} = \sum_{n=\text{even}} g_n(E) P_n(\xi) \quad , \quad (14a)$$

$$g_{\text{odd}} = \sum_{n=\text{odd}} g_n(E) P_n(\xi) \quad . \quad (14b)$$

The kinetic equations separate into an even part:

$$-i\omega g_{\text{even}} + ik_p A \{\xi g_{\text{odd}}\} - c(g_{\text{even}}) = -i\omega \Phi F_0 \quad , \quad (15a)$$

and an odd part:

$$A \{-i\omega g_{\text{odd}} + ik_p \xi g_{\text{even}} - c(g_{\text{odd}})\} = 0 \quad . \quad (15b)$$

The kinetic response function for the total density can then be computed using the same formula [Eq. (4)] as for the case without trapped particles. Even with 32 Legendre polynomials, the kinetic response function, for $\nu_e = 0.01\omega_L$, does not agree with the analytic collisionless result near zero real frequency unless the growth rate is taken to be fairly large $\text{Im}[\omega] = 0.5\omega_L$. For smaller growth rates there is damping due to numerical resolution error. The numerical damping problem does not resolve even for 64 Legendre Polynomials and erratic oscillation of the solution set in due to loss of precision for this case. These numerical difficulties will be simply avoided by using a large growth rate for the TGLF model fitting.

The TGLF moment equations with trapped particles and collisions are split into three sets of moments. For example the total density moment can be written⁷

$$N = \frac{1}{n_0} \int d^3v g = N^u(1) - N^u(f_t) + N^t(f_t) \quad . \quad (16)$$

The first moment is for untrapped particles over all velocity space. The second moment is for the untrapped particles over the trapped region. The first two are not physical moments but are a mathematical trick to split up the integral over the passing region into two terms. The physical untrapped particle density is then the difference of these two moments. The third moment is the trapped particle density moment over the trapped region. The three different types of moments are treated independently which allows for discontinuity of the distribution function at the trapped passing boundary. This approach makes it possible to achieve an accurate representation of the collisionless density response function with trapped particles for a system of equations with a small number of velocity moments.⁷ The building blocks of the TGLF equations are moments over a wedge in velocity space $|\xi| \leq f_t$ since even the full velocity space moment is just a wedge moment with $f_t = 1$. For the wedge moment equations it is natural to expand the distribution function in Legendre polynomials with a rescaled argument

$$g(f_t) = \sum_{n=0}^{N_{\max}} g_n(E) P_n(\xi/f_t) / f_t^{n+1} \quad . \quad (17)$$

The definition of the wedge moments is the same as Eq. (6) with the Legendre polynomials replaced by $P_n(\xi) \rightarrow P_n(\xi/f_t) f_t^n$.

Taking moments of Eq. (1) over the trapped wedge in velocity space gives the system of equations for the untrapped wedge moments

$$-i\omega N^u + i\omega f_t \Phi + i\omega_L U_{\parallel}^u = \nu_N \frac{(1-f_t^2)}{f_t^4} \Pi^u, \quad (18a)$$

$$-i\omega T^u + i\omega_L \left(q_T^u + \frac{2}{3} U_{\parallel}^u \right) = \nu_T \frac{(1-f_t^2)}{f_t^4} \Pi^u, \quad (18b)$$

$$-i\omega U_{\parallel}^u + i\omega_L \left(\Pi^u + f_t^2 T^u + f_t^2 N^u \right) = -\nu_{UV} U_{\parallel}^u - \nu_{UQ} q_T^u + \nu_U \frac{(1-f_t^2)}{f_t^4} \Theta^u, \quad (18c)$$

$$-i\omega q_T^u + i\omega_L \left(dR_{\parallel T}^{u,LF} + f_t^2 dR_{TT}^{u,LF} + \frac{2}{3} \Pi^u + \frac{5}{3} f_t^2 T^u \right) = -\nu_{QU} U_{\parallel}^u - \nu_{QQ} q_T^u + \nu_Q \frac{(1-f_t^2)}{f_t^4} \Theta^u, \quad (18d)$$

$$-i\omega \Pi^u + i\omega_L \left(\Theta^u + \frac{4}{5} f_t^2 q_T^u + \frac{4}{3} f_t^2 U_{\parallel}^u \right) = -\nu_{\Pi} \Pi^u, \quad (18e)$$

$$-i\omega \Theta^u + i\omega_L \left(dR_{\parallel\parallel}^{u,LF} + \frac{27}{35} f_t^2 dR_{\parallel T}^{u,LF} + \frac{9}{5} f_t^2 \Pi^u \right) = -\nu_{\Theta} \Theta^u. \quad (18f)$$

For $f_t=1$ this reduces to our previous result [Eq. (8)]. The collision terms multiplied by $(1-f_t^2)$ come from the derivative of the distribution function with respect to ξ at the trapped passing boundary. These boundary terms couple all of the Legendre polynomial moments together. The closure like Eq. (9) must be supplemented by setting the higher Legendre moment terms to zero in each equation. This choice can be justified by the fact that the collisional damping rate increase like $n(n+1)$, where n is the Legendre index. Hence, the higher Legendre index terms will damp away faster than the lower ones and only the lowest index collision term is retained for each equation.

The trapped particle moment equations follow from the even wedge moments with the odd moments set to zero and $k_{\parallel}=0$.

$$-i\omega N^t + i\omega f_t \Phi = \nu_N \frac{(1-f_t^2)}{f_t^4} \Pi^t, \quad (19a)$$

$$-i\omega T^t = \nu_T \frac{(1-f_t^2)}{f_t^4} \Pi^t, \quad (19b)$$

$$-i\omega \Pi^t = -\nu_{\Pi} \Pi^t. \quad (19c)$$

If solved as a linear eigensystem, these equations give three eigenvalues $-i\omega = (0, 0, -\nu_{\Pi})$. Hence, there is no damping of the trapped density N^t or total pressure temperature T^t .

Transforming from frequency to time this system of equations can be solved as an initial value system giving the solution

$$N^t - f_t \Phi = N_\infty^t - \frac{\nu_N}{\nu_\Pi} \frac{(1-f_t^2)}{f_t^4} \Pi_0^t e^{-\nu_\Pi t} \quad , \quad (20a)$$

$$T^t = T_\infty^t - \frac{\nu_T}{\nu_\Pi} \frac{(1-f_t^2)}{f_t^4} \Pi_0^t e^{-\nu_\Pi t} \quad , \quad (20b)$$

$$\Pi^t = \Pi_0^t e^{-\nu_\Pi t} \quad . \quad (20c)$$

The density and temperature have an impulse driven by the boundary coupling to the initial stress Π_0^t that is damped to an asymptotic value (N_∞^t, T_∞^t) that is a constant. The stress damps to zero. This solution is also the solution of the system of equations

$$\frac{\partial}{\partial t} (N^t - f_t \Phi) = -\nu_\Pi (N^t - f_t \Phi - N_\infty^t) \quad , \quad (21a)$$

$$\frac{\partial}{\partial t} T^t = -\nu_\Pi (T^t - T_\infty^t) \quad , \quad (21b)$$

$$\frac{\partial}{\partial t} \Pi^t = -\nu_\Pi \Pi^t \quad . \quad (21c)$$

This form of the equations will be called the ‘‘transferred damping’’ form since the damping of the stress has been transferred to the density and temperature equations through the trapped boundary terms. Transforming this system to frequency gives the eigenvalues characteristic of the damping of the initial impulse $-i\omega = (-\nu_\Pi, -\nu_\Pi, -\nu_\Pi)$ whereas the original moment equations gave eigenvalues characteristic of the asymptotic solution. A similar analysis of the untrapped wedge moment equations [Eq. (18)] gives the same transferred damping form for the boundary terms for the even moments. The odd moments also pick up transferred damping terms from their trapped boundary coupling. If higher Legendre polynomial terms are kept, then there are more trapped boundary terms in all of the equations. The boundary terms all have the property that they have the overall factor $(1-f_t^2)$ that vanishes when all of the particles are trapped $f_t=1$. The closure strategy will be to add transferred damping terms to replace the trapped boundary terms. The optimal values obtained for the no-trapped particle case will be used for the collision coefficients that are not from the trapped boundary. A simple form of this model for the trapped boundary collision effects for the trapped particles is

$$-i\omega(N^t - f_t \Phi) = -\nu_B (1-f_t^2) (N^t - f_t \Phi - N_\infty^t) \quad , \quad (22a)$$

$$-i\omega T^t = -\nu_B (1-f_t^2) (T^t - T_\infty^t) \quad , \quad (22b)$$

$$-i\omega \Pi^t = -\nu_\Pi \Pi^t - \nu_B (1-f_t^2) (\Pi^t - \Pi_\infty^t) \quad . \quad (22c)$$

A boundary term has been added to the stress equation to account for the coupling to higher velocity moments neglected in Eq. (19). This is the form used for all of the TGLF collision models to date. The coefficient ν_B is optimized to fit exact initial value gyro-kinetic results. There are three versions that have been developed with different asymptotic limits. The first two were hand fit to a database of linear gyrokinetic stability runs primarily for trapped electron modes over a range of parameters. The full toroidal equations were used for the fitting. The resulting models are as follows:

Model 0:

$$N_{e\infty}^t = -f_t \Phi, \quad T_{e\infty}^t = 0, \quad \Pi_{e\infty}^t = 0, \quad \nu_B = \nu_e \frac{\Lambda_1}{1 + \Lambda_2 (\nu_e / \omega_{de})}, \quad (23a)$$

$$\Lambda_1 = 3.1 \left\{ k_i \text{Max} \left[0.36 + 0.1 \frac{R}{L_{ne}}, 0.0 \right] + \text{Max} \left[\frac{R}{L_{ne}} + 10.8, 1.8 \right] \left[1.5 \left(1 - \text{Tanh} \left[\left(\frac{R}{12.6 L_{ne}} \right)^2 \right] \right) \right] \right\}, \quad (23b)$$

$$\Lambda_2 = (2.1 k_i + 8.0 k_i^2) (\nu_e / \omega_{de}). \quad (23c)$$

Model 1:

$$N_{e\infty}^t = 0, \quad T_{e\infty}^t = 0, \quad \Pi_{e\infty}^t = 0, \quad \nu_B = \nu_e \frac{\Lambda_1}{1 + \Lambda_2 (\nu_e / \omega_{de})}, \quad (24a)$$

$$\Lambda_1 = 3.79 \left\{ 0.41 + 0.7 \left(\frac{k_i}{k_{s0}} \right)^{1.7} (1.0 + 1.4 k_i / 0.38) \left(1.0 + \left(\frac{k_i}{0.38} \right)^4 \right) \right\}, \quad (24b)$$

$$\Lambda_2 = 4.63 k_i \nu_e / \omega_{de}. \quad (24c)$$

where for both models $k_i = k_y \sum_{a=\text{ions}} (T_a m_a n_a Z_a / T_0 m_0 n_e) / \sum_{a=\text{ions}} (n_a Z_a / n_e)$, $k_{s0} = k_y \sqrt{T_a m_a / T_0 m_0}$, $k_y = (nq/r) [\sqrt{T_0 / m_0} / (eB_0 / m_0 c)]$, $R / L_{ne} = -(R / ne)(dne/dr)$, $\omega_{de} = (k_y / R) T_e B_0 / (T_0 B) \sqrt{T_0 / m_0}$ with T_0 , B_0 , m_0 the units of temperature, magnetic field and mass.

The main difference between these two models is the asymptotic density limit $N_{e\infty}^t$. Both use the electron curvature drift at the outboard mid-plane ω_{de} as a reference frequency since this is the resonant frequency in the toroidal trapped electron moment equations. Neither model was fit to non-linear gyrokinetic turbulence simulations. The models are not robust in that they required corrections for parameters $(R / L_{ne}, k_y)$ other than the normalized collision frequency ν_e / ω_{de} . Only model 1 was used for prediction of experimental transport⁸ since it does not require density gradient corrections. After construction of these models, non-linear GYRO runs were performed. A comparison of model 1 used in TGLF (circles) with GYRO results (squares) is shown in

Fig. 2. The main defect appears to be that the large collision frequency residual of the ion thermal transport is too large. The model-1 particle flux [Fig. 2(c)] also reduces to the GYRO result without any trapped particles (triangles) rather than the correct GYRO case with trapped particles. Similar results are obtained for model-0. The high collision frequency residual energy fluxes are hard to match since they remain well above the no-trapped electron value for the fluxes [triangles in Fig. 2(a,b) for GYRO]. In both models, the boundary term becomes independent of collision frequency $\nu_B \rightarrow \omega_{de} \Lambda_1 / \Lambda_2$ for large ν_e . This determines the residual effect on the fluxes and prevents the energy fluxes from reducing to the no-trapped particle level. The truncation case of the circulating particle collision coefficients in Table I were used in these two models but substituting the optimized coefficients does not change the results significantly.

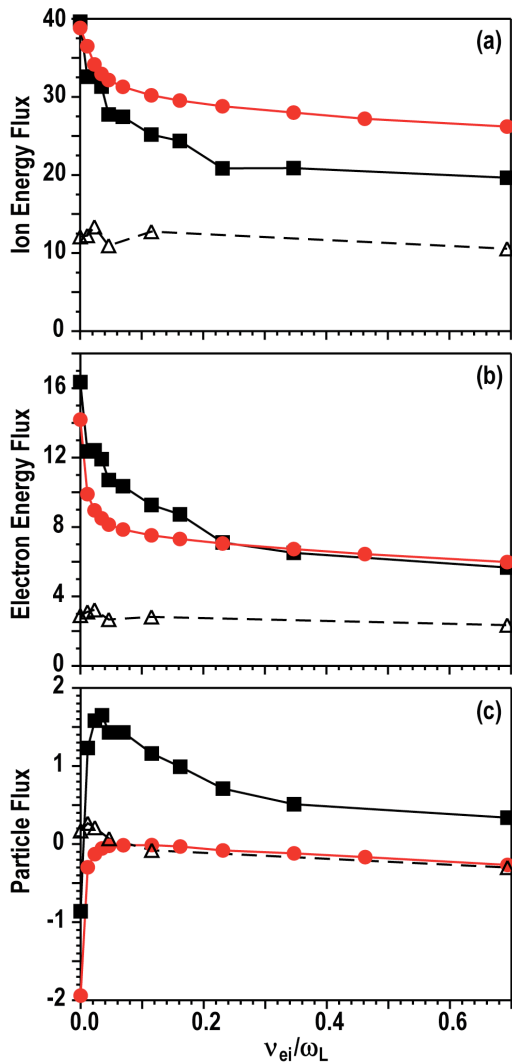


Fig. 2. Ion energy flux/ $(n_e T_e c_s \rho_s^2 / a^2)$ (a), electron energy flux/ $(n_e T_e c_s \rho_s^2 / a^2)$ (b) and electron particle flux/ $(n_e c_s \rho_s^2 / a^2)$ (c) for the GA-STD case [Eq. (27)] vs. ν_{ei}/ω_L for GYRO (squares), TGLF model-1 (circles) and for GYRO without trapped particles (triangles).

The main topic of this paper is a new collision model (model 2). It still has the same transferred damping form [Eq. (22)] but is fit to the kinetic solution in the slab limit with the bounce averaging model described above. As mentioned before, the Landau resonance frequency

is the largest frequency in the equation for the circulating electrons at ion-scale poloidal wavelengths. If k_{\parallel} is set to zero, then there is no collisional damping of the g_0 moment (density, temperature, etc.) in the kinetic model [Eq. (15)]. This must also be true when there are trapped particles. The trapped particle density gets damped through transfer from the boundary connection to circulating particles, but if there is no parallel wavenumber, then even the circulating particle density is not damped by collisions. Hence the model for the boundary transfer terms in the trapped particle equations should have the property that the coefficient ν_B vanishes when $k_{\parallel} \rightarrow 0$. For a power law form, this gives $\nu_B \propto \omega_L (\nu_e / \omega_L)^\alpha$ with $1 > \alpha > 0$. Taking $\nu_B \propto \sqrt{\nu_e \omega_L}$ is found to be nearly optimal for fitting TGLF to the kinetic response function. Already this new model departs from the previous ones by identifying the Landau frequency as the reference frequency for the model rather than the curvature drift frequency.

Asymptotic in time is the same as the large collision frequency limit for the kinetic equations. Taking the density moment of the distribution function over just the trapped region for the solution to the kinetic model with trapped particles [Eq. (15)], and comparing it with the density moment over the trapped region for the solution to the kinetic model without trapped particles [Eq. (1)], it is found that the two moments become nearly equal to each other for large collision frequency. Thus, the asymptotic trapped particle density limit is the projection to the trapped region of the distribution function without trapped particles or bounce averaging. Taking into account the different Legendre Polynomial arguments and truncating the higher moments, the mapping between the asymptotic trapped moments and the $f_t = 1$ wedge moments is

$$N_{\infty}^t(f_t) = N_{\infty}^u(f_t) = f_t N^u(1) - \frac{3}{4} f_t (1 - f_t^2) \Pi^u(1) \quad , \quad (25a)$$

$$T_{\infty}^t(f_t) = T_{\infty}^u(f_t) = f_t T^u(1) - \frac{1}{2} f_t (1 - f_t^2) \Pi^u(1) \quad , \quad (25b)$$

$$\Pi_{\infty}^t(f_t) = \Pi_{\infty}^u(f_t) = f_t^3 \Pi^u(1) \quad . \quad (25c)$$

These are the asymptotic terms in Eq. (22) for the new model (model-2). Since both the trapped moments and the wedge untrapped moments over the trapped region have the same asymptotic limit, the physical total moments [Eq. (16)] approaches just the $f_t = 1$ moment. A similar asymptotic limit model was tried for the odd moments of the circulating distribution function in the trapped wedge. The numerical optimization set the coefficients of the odd boundary transfer terms to zero so these terms will not be presented in detail.

An excellent fit (5.2% fractional deviation average over $\nu_e / \omega_L = 0.01, 0.05, 0.5$ to the kinetic response of the total density can be obtained using the asymptotic limits Eq. (25) in Eq. (22), for the numerically determined value of $\nu_B = 1.55 \sqrt{k_p \nu_{ei}}$ for $Z_{eff} = 1$. An example of the fit is shown in Fig. 3. The deviation is low partly because the growth rate is large so the poles of the TGLF response function are far below the real frequency axis. Lowering the growth rate increases the deviation and gives a larger optimized fit coefficient. This increase is due to

the spurious numerical damping of the trapped particles that gets stronger at low collision frequency, growth rate and real frequency.

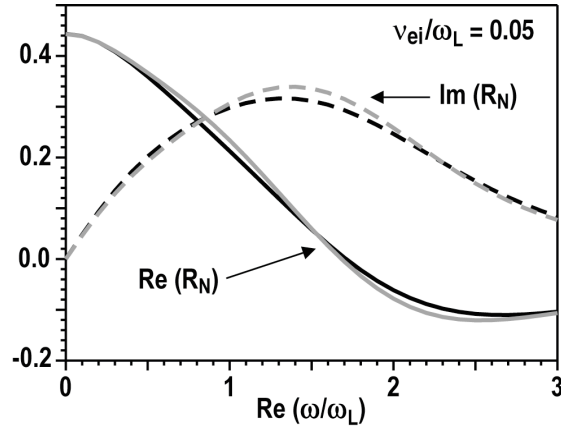


Fig. 3. Real (solid) and imaginary (dashed) parts of the density response function for $\nu_{ei}/\omega_L = 0.05$, showing kinetic solution with 32 Legendre polynomials (black) and TGLF model-2 with optimized fit (gray).

Unfortunately, the numerically optimized fit to the kinetic model does not agree with the non-linear GYRO simulation fluxes. However, simply adjusting the leading constant down by a factor of 10.1 does give good agreement with GYRO as shown in Fig. 4. It appears that the kinetic model matches the asymptotic behavior and the square root of the collision frequency dependence of the trapped boundary terms, but gives too strong a coupling. This may be due to the use of global Legendre polynomials, since this makes all of the derivatives of the distribution function continuous at the trapped-passing boundary. Other numerical schemes, besides Legendre polynomials, and other models for the bounce averaging effect, have been tried for the kinetic model but none resulted in a good fit to GYRO without adjustment. More complicated versions of the TGLF model were also tried, some giving improved agreement with the kinetic model, but none improved agreement with GYRO. The bottom line is that it does not really matter if the kinetic model of bounce averaging is good, what ultimately matters is if the TGLF collision model gives a good fit to GYRO. Using the form of the TGLF model above which was determined by studying the properties of the kinetic equations, a good fit to GYRO is obtained with the coefficients

Model-2:

$$\nu_B = 0.114 \sqrt{\nu_{te} k_{\parallel} \nu_e (1 + 0.82 Z_{eff})} . \quad (26)$$

The Z_{eff} dependence has been found by fitting to GYRO with $Z_{eff} = 0, 1.0$. Collision frequency scans of the GA-STD case (see the next section) were used for this fitting. The $Z_{eff} = 1.0$ case is

shown in Fig. 4 . Since the new model-2 is fit to a collision scan from GYRO rather than an exact kinetic solution it must be verified with more GYRO runs that were not used for the fit.

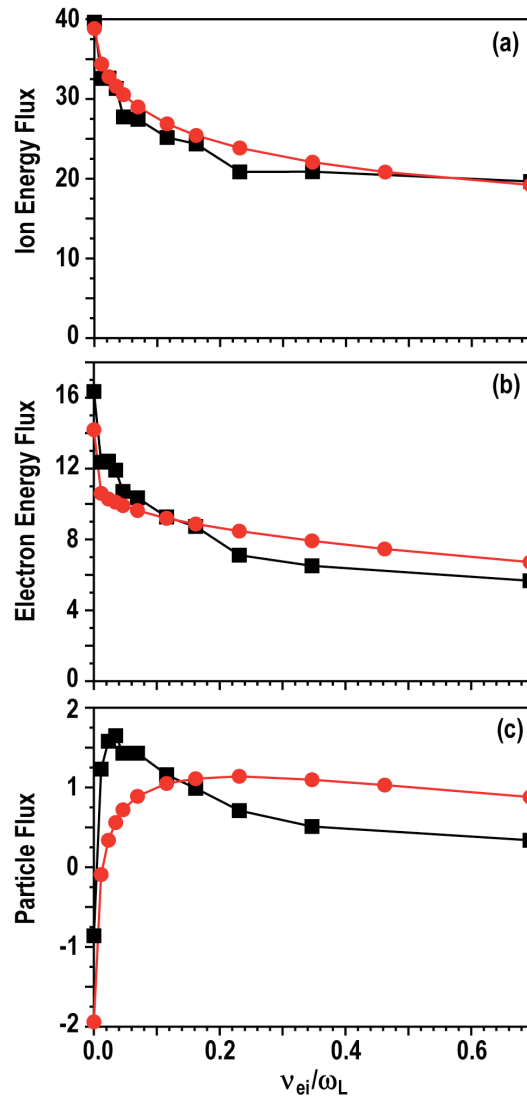


Fig. 4. Ion energy flux/ $(n_e T_e c_s \rho_s^2 / a^2)$ (a), electron energy flux/ $(n_e T_e c_s \rho_s^2 / a^2)$ (b) and electron particle flux/ $(n_e c_s \rho_s^2 / a^2)$ (c) for the GA-STD case [Eq. (27)] vs. v_{ei}/ω_L for GYRO (squares), TGLF model-2 (circles).

IV. VERIFICATION WITH GYRO AND VALIDATION WITH EXPERIMENT

This new TGLF model [Eqs. (22), (25), (26)] has been extensively verified with 64 GYRO non-linear turbulence simulations with collisions. The runs were grouped as scans around two reference points.

$$\text{GA-STD: } R/a=3, r/a=0.5, q=2, \hat{s}=1, a/L_{T_e} = a/L_{T_i} = 3, a/L_{n_e} = a/L_{n_i} = 1, \\ T_e = T_i, n_e = n_i, \beta=0, \hat{v}_e=0, \kappa=1, s_k=0, \delta=0, s_\delta=0 \quad . \quad (27)$$

$$\text{LM01: } \text{STD+ } r/a=0.5, a/L_{T_{e,i}} = 2.0, \kappa=1.5, s_\kappa=0.17, \hat{v}_e=1.0 \quad . \quad (28)$$

The parameters changed from these reference points for each scan are given in Table II. The GYRO normalization convention $\hat{v}_e = v_e a / \sqrt{T_e / m_i}$ is used.

Table II
GYRO Parameter Scan Details

Scan	Case	Scanned Parameters	Runs
55	STD	q -scan, $q=1.5$ – 4.0 , with $\hat{v}_e=1.0$	4
56	STD	q -scan, $q=2.0$ – 5.0 , with $\hat{v}_e=0.1, 1.0$, $r/a=0.75$	8
58	STD	a/L_T -scan, $a/L_T=2.0$ – 4.0 @ $\hat{v}_e=0.1$, $a/L_T=1.5$ – 4.0 @ $\hat{v}_e=1.0$	11
60	STD	\hat{v}_e -scan, $\hat{v}_e=0.0$ – 3.0 @ $r/a=0.5$, $\hat{v}_e=0.0$ – 0.2 @ $r/a=0.75$	16
62b	STD	r/a -scan, $r/a=0.01$ – 1.0 @ $\hat{v}_e=1.0$	5
70	LM01,	q -scan, $q=2$ – 5 , @ $\hat{v}_e=0.1, 1.0$	11
72	LM01	\hat{v}_e -scan, $\hat{v}_e=0.0$ – 1.5	9

All of the GYRO runs used the same grid resolution with 16 mode numbers $0 \leq k_y \leq 0.75$ where and n is the toroidal index, ρ_s is the reference gyroradius. A box size of $[L_x/\rho_s, L_y/\rho_s]=[126, 126]$ and $n_r=170$ radial grid points were used. The fractional deviation of the TGLF effective diffusivities from GYRO for each scan are charted in Fig. 5. In each scan the new collision model (model-2) is better than model-1. The average deviations $[\chi_i, \chi_e]$ for the whole dataset of 64 cases dropped from $[0.24, 0.27]$ for model-1 to $[0.10, 0.13]$ for model-2. The collision frequency scan at the STD point used to fit the overall coefficient of the boundary terms is included in scan 60. Scan 58 changes the temperature gradients together and the two LM01 scans (70,72) change the base geometry shaping compared to the STD cases. The other scans are all either q -scans or r/a scans in order to verify the two main dependencies in the TGLF boundary model ($k_{\parallel} \propto 1/Rq$, $f_t \approx \sqrt{2r/R}$, for $r/R \ll 1$). The effective thermal diffusivity as a function of aspect ratio (scan 62b) and q (scan 55) are shown in Fig. 6 for the

STD case with $\hat{v}_e = 1.0$. The new model-2 tracks the GYRO results very well but model-1 has the wrong slope in both parameters.

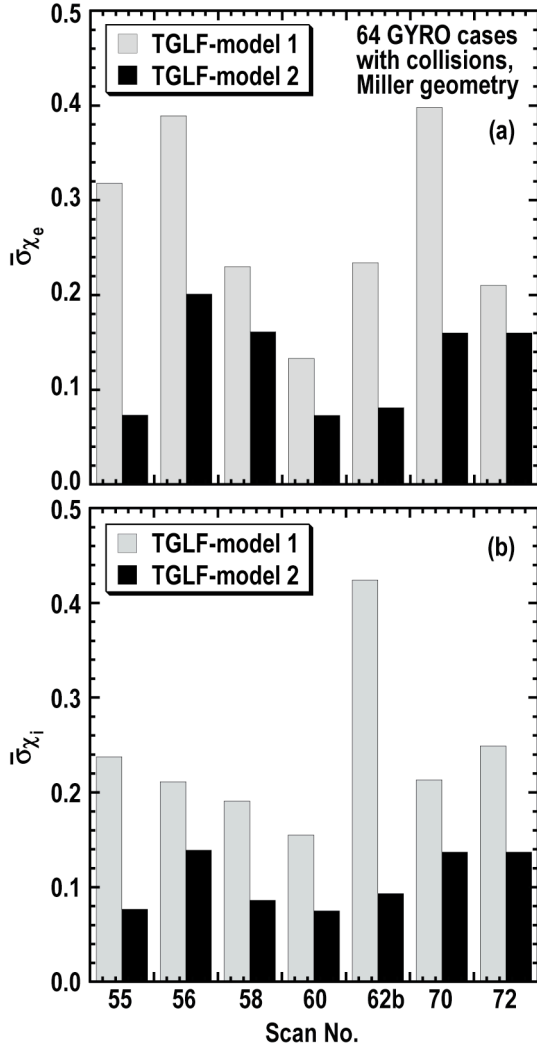


Fig. 5. Bar chart of fractional deviation between TGLF and GYRO effective electron (a) and ion (b) energy diffusivities (i.e. flux/gradient). Statistics for model-1 are in gray and model-2 are in black.

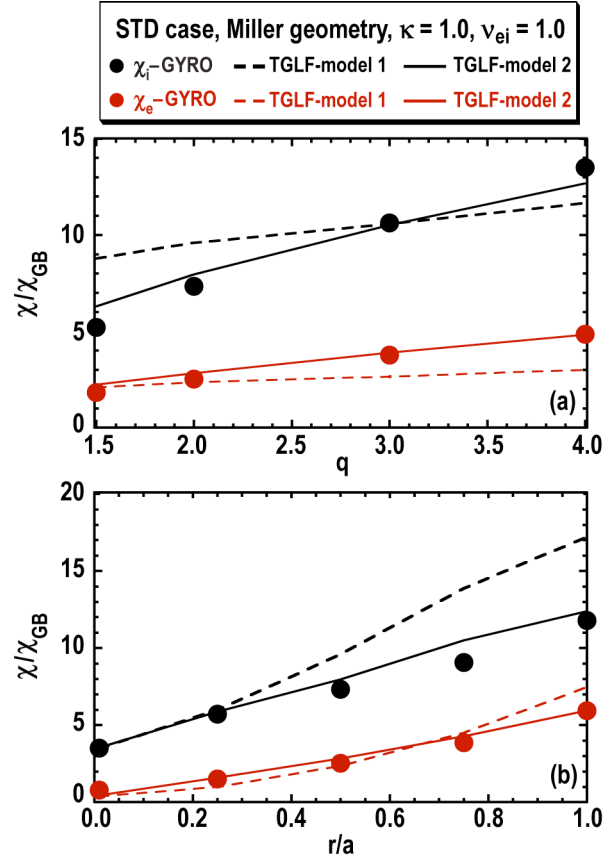


Fig. 6. q -scan (a) and r/a scan (b) around the GA-STD point showing electron (gray) and ion (black) effective thermal diffusivities for GYRO (circles), TGLF-model-1 dashed, and TGLF-model-2 solid.

The new collision model has been tested with experimental data using the large tokamak database (96, L-modes and H-modes, from DIII-D, JET, TFTR) of Ref. 8. Figure 7 shows the predicted versus experimental incremental stored energy for the 96 discharges using TGLF with the new collision model (TGLF-model-2). We find the statistical average of the rms deviation of the TGLF predicted temperatures from the $q=1$ surface to $\rho=0.84$ show very little change from the TGLF-model-1 results published in Ref. 8. The rms error in W_{inc} is 21% with an effective

offset of $\langle R_w \rangle - 1 = 2\%$. The corresponding average rms errors in (T_i, T_e) for model-2 are [15%,16%] and differ from the model-1 values by less than 0.5%.

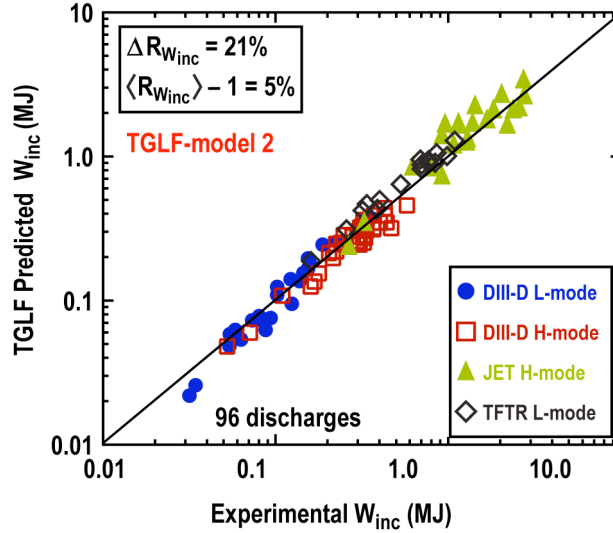


Fig. 7. Predicted incremental stored energy W_{inc} from TGLF-model-2 vs. experimental W_{inc} for 96 L- and H-mode discharges.

Looking in detail at a dedicated experiment¹⁴ designed to change the collisionality while keeping other dimensionless plasma parameters important to gyro-kinetic turbulence fixed does show a difference between the two models. The ion and electron temperature deviation σ_T and offsets f_T defined by

$$\sigma_T = \sqrt{\frac{1}{N} \sum_{j=1}^N \varepsilon_j^2} / T_{rms}^{EXP}, \quad f_T = \frac{1}{N} \sum_{j=1}^N \varepsilon_j / T_{rms}^{EXP}, \quad (29a)$$

where

$$T_{rms}^{EXP} = \sqrt{\frac{1}{N} \sum_{j=1}^N (T_j^{EXP})^2} \quad \text{and} \quad \varepsilon_j = T_j^{TGLF} - T_j^{EXP}, \quad (29b)$$

are shown in Fig. 8 for the three DIII-D L-mode discharges comprising a factor of eight scan in ν^* . The new collision model has a lower deviation from the data than model-1. The old model clearly exhibits a trend in the offsets changing from negative (predicted temperature low) to positive (predicted temperature high) as ν^* is decreased. That trend is still present in the new model but to a lesser extent. There may be some contribution to this trend from the simple Chang-Hinton¹⁵ ion thermal neoclassical diffusivity model used. There was also a pair of H-modes in the experiment of Ref. 14. For the DIII-D H-mode ν^* scan we observed little change in the predicted profiles when the collision model is changed in TGLF. For both H-mode cases, the ExB shear has suppressed the low- k modes resulting in the ion thermal transport being close to neoclassical and the electron thermal transport being dominated by ETG modes. Since the

change in the collision model impacts mainly the low- k modes, which are stable in the H-mode pair, the insensitivity to the collision model is not unexpected. Overall, we find that improving the agreement of TGLF with GYRO also improved the agreement with experiment. This is a positive indication that the drift-wave turbulence being modeled is contributing to the transport in tokamaks.

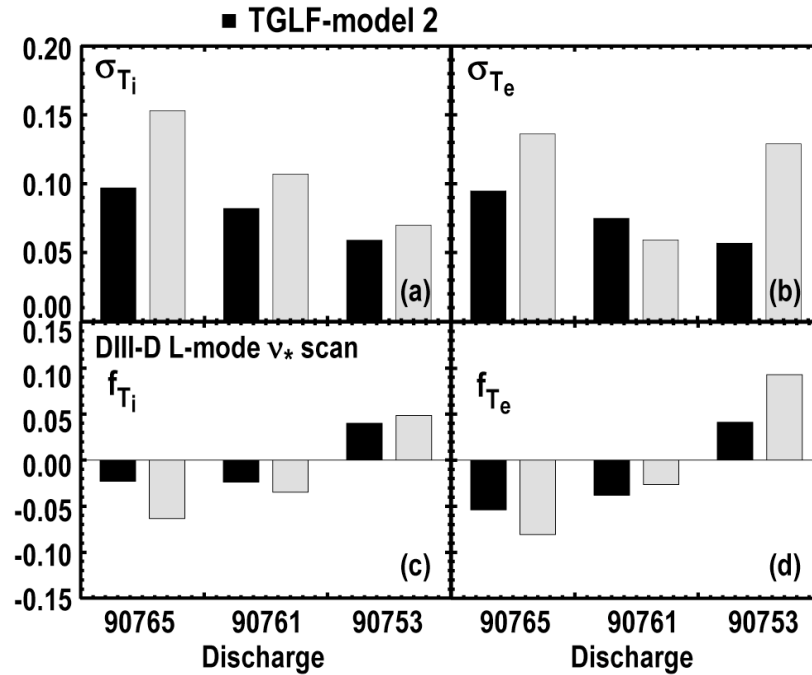


Fig. 8. RMS error and offset in the ion (a,c) and electron (b,d) temperature profiles vs. discharge using the TGLF-model-1 (gray) and TGLF-model-2 (black) models for a DIII-D L-mode collisionality scan. Discharges 90765 and 90753 correspond to the high and low collisionality cases respectively.

V. SUMMARY

In this paper a new model for electron collisions in the TGLF equations has been developed. The new model (model 2) consists of numerically optimized collision coefficients (Table I) for the circulating electron equations [Eq. (10)] and the transferred damping form [Eq. (22)] of the trapped-passing boundary terms with new asymptotic limits [Eq. (25)] and a simpler coefficient [Eq. (26)]. The goal was to solve the local gyro-kinetic equation for the fluid moment perturbation response functions (density, pressure, parallel flow, parallel energy flux) numerically with pitch angle scattering collisions. This would then be used to fit a reduced model for the TGLF equations. This goal was realized for the case without trapped particles resulting in a modest improvement of the TGLF model for the circulating particle sector. Extending this to trapped particles proved difficult due to the need to introduce a model for the bounce averaging of the Landau resonance by the trapped particles. Fitting TGLF to the kinetic response functions resulted in a collisional damping of trapped electrons that was too strong. However, a simple adjustment of the overall strength of the trapped boundary coefficient did result in a good fit of TGLF fluxes to GYRO nonlinear simulations. The kinetic model informed the physics choices for the TGLF model in several ways that led to success. The first was the observation that the Landau resonance frequency of the passing electrons is the largest frequency and it sets the scale for the collision frequency. Thus, the natural dimensionless parameter for gyro-kinetic collisions is not the neoclassical collisionality ν^* but is the ratio of the electron collision frequency to the electron Landau resonance frequency $\nu_e^L = \nu_e / \omega_L \cong \nu_e \pi R / \sqrt{2T_e / m_e}$, where an estimation of the parallel wavenumber has been used $k_{\parallel} = (-i/Rq)(\partial/\partial\theta) \approx 1/(R\pi)$. Secondly, the kinetic theory showed the trapped boundary terms were all proportional to the factor $(1 - f_i^2)$. Third, the trapped boundary terms should have no effect if the parallel wavenumber is zero constraining the trapped boundary model coefficient (ν_B) to be proportional to $\omega_L (\nu_e / \omega_L)^\alpha$ with $1 > \alpha > 0$. Finally, the large collision frequency limit of the kinetic model determined the asymptotic limit for the TGLF model to be the projection of the passing particle distribution without trapping to the trapped region [Eq. (25)]. These four physics constraints determined the transferred damping form of the TGLF trapped boundary model [Eq. (22)] up to three fitting parameters (one for $Z_{eff} = 0$ and one for $Z_{eff} > 0$ and the exponent α). The kinetic equation with a specific bounce averaging model did not yield the correct strength, but did give the correct exponent ($\alpha = 0.5$). Direct fitting to GYRO fluxes was possible for the last two parameters. The new model captures the correct dependence on the primary parameters ($q, r/R$) that it depends upon as validated by non-linear GYRO simulations. The new model was found to improve the agreement of TGLF predicted temperatures with experiment for dedicated collision frequency scans.

REFERENCES

- ¹G. W. Hammett and F. W. Perkins, Phys. Rev. Lett. **64**, 3019 (1990).
- ²R. E. Waltz, R. R. Dominguez, and G. W. Hammett, Phys. Fluids B **4**, 3138 (1992).
- ³W. Dorland and G. W. Hammett, Phys. Fluids B **5**, 812 (1993).
- ⁴M. A. Beer and G. W. Hammett, Phys. Plasmas **3**, 4046 (1996).
- ⁵M. A. Beer and G. W. Hammett, Phys. Plasmas **3**, 4018 (1996).
- ⁶R. E. Waltz, G. M. Staebler, W. Dorland, G. W. Hammett, M. Kotschenreuther, and J. A. Konigs, Phys. Plasmas **4**, 2482 (1997).
- ⁷G. M. Staebler, J. E. Kinsey, and R. E. Waltz, Phys. Plasmas **12**, 102508 (2005).
- ⁸J. E. Kinsey, G. M. Staebler, and R. E. Waltz, Phys. Plasmas **15**, 055908 (2008).
- ⁹M. Kotschenreuther, G. Rewoldt, and W. M. Tang, Comput. Phys. Commun. **88**, 128 (1995).
- ¹⁰J. Candy and R. E. Waltz, J. Comp. Physics **186**, 545 (2003).
- ¹¹T. M. Antonsen, Jr. and B. Lane, Phys. Fluids **23**, 1205 (1980).
- ¹²S.P. Hirshman and D. J. Sigmar, Phys. Fluids **19**, 1532 (1976).
- ¹³P.J. Catto, K. T. Tsang, J. D. Callen, and W. M. Tang, Phys. Fluids **19**, 1596 (1976).
- ¹⁴C. C. Petty and T. C. Luce, Phys. Plasmas **6**, 909 (1999).
- ¹⁵C.S. Chang, Phys. Fluids **26**, 2140 (1983).

ACKNOWLEDGMENT

This work supported by the U.S. Department of Energy under DE-FG02-95ER54309.